Extending the LCSR method to the electromagnetic pion form factor at low momenta using QCD renormalization-group summation

César Ayala, ^{1,*} S. V. Mikhailov, ^{2,†} and A. V. Pimikov^{2,‡}

¹Departamento de Ingeniería y Tecnologías, Sede La Tirana,

Universidad de Tarapacá, Av. La Tirana 4802, Iquique, Chile

²Bogoliubov Laboratory of Theoretical Physics, JINR, 141980 Dubna, Russia

(Dated: May 27, 2025)

We obtain the electromagnetic pion form factor (emFF) F_{π} for spacelike mid-range of momentum transfer in QCD. We use renormalization group summation within the light cone sum rules (LCSRs) to obtain the QCD radiative corrections to the F_{π} and involve contributions of the leading twist 2 and twists 4, 6. The strong coupling constants in this approach are free of Landau singularities, which allows one to go down to the lower transferred momentum Q^2 . The prediction of the calculations performed reproduces the experimental data below/around $Q^2 = 1 \text{ GeV}^2$ significantly better than analogous predictions based on a fixed-order power-series expansion in the standard QCD.

I. INTRODUCTION

The hadron form factor (FF) is the appropriate candidate to test the QCD in the meaningful range of the transferred momentum, e.g., [1]. When we delve into the mid- to low-energy range, the properties of analyticity and unitarity in QCD come to the forefront. These properties guide us toward the light cone sum rule (LCSR) and dispersion relations [2–4], shaping our understanding of this energy range. Let us delve into the pion electromagnetic FF (emFF), which is essentially a parametrization of the four-vector part of the expectation value of the electromagnetic current

$$\langle \pi^+(p_2) | j_{\mu}^{em} | \pi^+(p_1) \rangle = (p_1 + p_2)_{\mu} F_{\pi}(q^2), q = p_1 - p_2.$$
 (1)

As we mentioned, the dispersion relation is crucial to extend the analyticity structure of this physical quantity. To this end, we will invoke the obtained knowledge of the pion transition FF (TFF) [5] because of their analogy, i.e., the replacing axial current $j_{\mu 5}$ with electromagnetic one j_{μ}^{em} in the corresponding LCSR where the dominance on the light cone leaves to an expansion in nonlocal operators and then to pion distribution amplitudes (DAs) $\varphi_{\pi}(x)$. We will follow the LCSRs as a general frame to obtain the emFF without appealing to an additional ansatz/suggestion about the effective scale μ^2 of the QCD coupling constant $a_s(\mu^2) = \alpha_s(\mu^2)/(4\pi)$ after borelization (see upper way in Fig.1). The $O(\alpha_s)$ corrections to the LCSR for the emFF within fixed-order perturbation theory (FOPT) were calculated for the first time in [3]. Then, the LCSR was updated from different aspects in [4, 6]. We use the experimental data from the JLab collaboration in [7] and that cover the intermediate energy range $0.6 \le (-q^2 = Q^2) \le 2.45 \text{ GeV}^2$, which is well suited for testing the approach above. The meaningful analysis of this data processing and the results for the intrinsic pion structure were presented in [8] and [6]. To be more consistent, we start with the initial object to construct the corresponding LCSR – the correlation amplitude $T_{\mu\nu}$,

$$T_{\mu\nu}(p,q) = i \int d^4z \, e^{iqz} \langle 0|T \left\{ j_{\mu 5}^+(0) \, j_{\nu}^{em}(z) \right\} |\pi^+(p)\rangle \,; \tag{2a}$$

$$j_{\mu 5}^+(0) = \bar{d}(0)\gamma_\mu\gamma_5 u(0), \ j_\nu^{em}(z) = e_u\bar{u}(z)\gamma_\nu u(z) + e_d\bar{d}(z)\gamma_\nu d(z) - \text{ the quark electromagnetic current}. \ \ (2b)$$

^{*}Electronic address: cayalan@academicos.uta.cl

[†]Electronic address: mikhs@theor.jinr.ru

[‡]Electronic address: pimikov@mail.ru

The correlator $T_{\mu\nu}$ serves to extract the emFF F_{π} and can be presented as the expansions both in twists and in PT series [4],

$$T_{\mu\nu}(p,q) \to i f_{\pi} 2p_{\mu} p_{\nu} \left(T_{(\text{tw}2)} \otimes \varphi_{\pi}^{(2)} + T_{(\text{tw}4)} \otimes \varphi_{\pi}^{(4)} + T_{(\text{tw}6)} \right);$$
 (3a)

$$T_{(\text{tw2})}(Q^2, \sigma; x) = \sum_{k=0} a_s^k(\mu^2) T^{(k)}(x),$$
 (3b)

where the sign \otimes means the convolution $A \otimes B = \int_0^1 dx A(x) B(x)$; $-q^2 = Q^2, -(p-q)^2 = \sigma$; the upper index (k) numerates orders of a_s . Rearrangement and summation by the renormalization group (RG) of the amplitude $T_{\text{(tw2)}} \otimes \varphi_{\pi}^{(2)}$ in Eq.(3b) are discussed in Sec.II, and some results for the LCSR amplitude $T^{(1)}(x)$ are outlined in Appendix A.

Conceptually, the consideration here follows our previous analysis of a somewhat similar object – the pion TFF in [5, 9-11], with the goal to improve the results of FOPT by involving a renormalization group and to extend the LCSR method to smaller transfer momentum Q^2 . In what follows we will hold the methodical correspondence between the pion TFF and the pion emFF. Moreover, we will use nonperturbative inputs in our emFF calculations that correspond to the results for every twist in the phenomenological analysis for the pion TFF in [11] because of their universal character. It is instructive to follow the general blockdiagram of this kind of calculations in Fig. 1, wherein the standard FOPT LCSR approach is shown in the upper line for the comparison with ours in the lower line. Below, we briefly discuss the contents of the blocks and their relations.

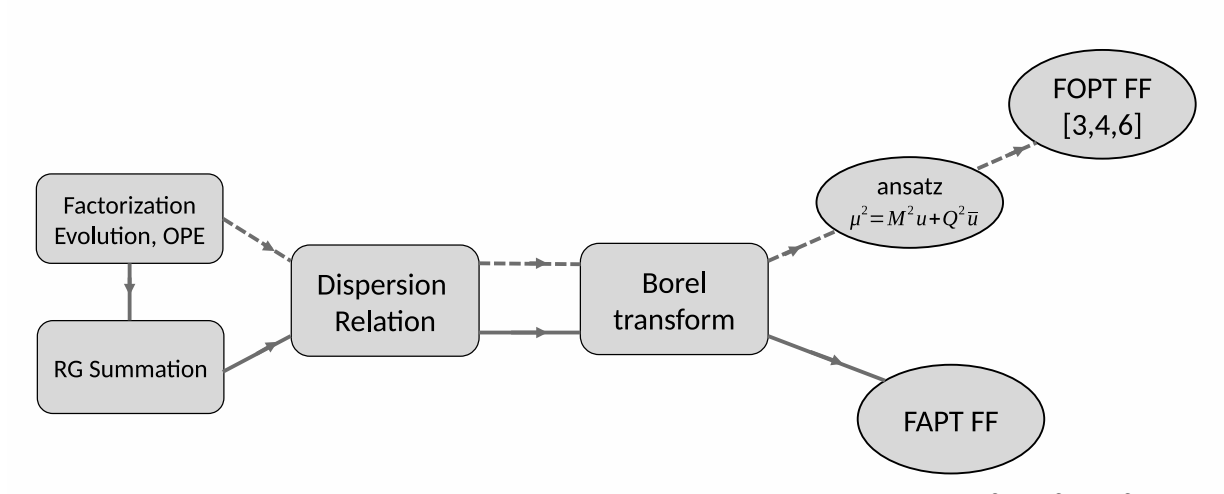


FIG. 1: The upper dashed line connected blocks show the way of the standard FOPT LCSR, here $\mu^2 = \mu_F^2 = \mu_R^2$ is renormalization/factorization scale, M^2 is the Borel parameter. The lower solid line illustrates our approach to the LCSR with the preliminary renormalization group summation.

Application of the dispersion relation to the amplitudes that were already RG-summed naturally transforms the power series in the QCD running coupling \bar{a}_s^{ν} (see Eq.(A4a)), $\bar{a}_s = \bar{\alpha}_s/(4\pi)$ to the non-power series of Fractional Analytic Perturbation Theory (FAPT) with three coupling constants $\{A_{\nu}, \mathfrak{A}_{\nu}, \mathcal{A}_{\nu}\}$ [5, 9–11], which are the corresponding images of \bar{a}_s^{ν} : A_{ν} is the spacelike image of \bar{a}_s^{ν} , \mathfrak{A}_{ν} is the timelike one, and \mathcal{I}_{ν} is their further generalization. Just this kind of generalization of the coupling constant, $\mathcal{I}_{\nu}(y,x)$, appears due to the action of "subtraction of continuum" [5, 9], which is a characteristic of the usual LCSR technique. The considered FAPT coupling constants are bounded from above (except singularity in vicinity of $\mu^2 = 0$ at $\nu < 1$) and have no Landau singularities at $\mu^2 = \Lambda_{\rm QCD}^2$ [12, 13] in contrast to the standard QCD $\bar{a}_s(\mu^2)$, see the detailed discussion in Appendix B. These features of the FAPT couplings allow one to extend the perturbative analysis well below the conventional pQCD boundary $\mu_0^2 = 1$ GeV².

These considerations applied to the leading order of twist 2 are the subject of Sec.III, while the required important technical results of FAPT are collected in Appendix B, which can be considered as an independent compendium of the existing, useful FAPT results. The formulas for the Borel transformation necessary to carry on the analysis are presented in Appendix C. The Borel image of the running coupling \bar{a}_s versus the μ -ansatz [3, 4, 6] (see upper line

in Fig.1) is discussed in part there. In Sec. IV and in Appendix D, the same approach to the LCSR as for twist 2 are applied to the amplitude $T_{(\text{tw4})} \otimes \varphi_{\pi}^{(4)}$ of twist 4. In Sec. V, we discuss important nonperturbative inputs for the LCSR (see also Appendix E) that significantly affect the result. Finally, we provide our predictions for the emFF $F_{\pi}^{\text{LCSR}}(Q^2)$ in comparison with the experimental data.

II. RG SUMMATION FOR THE TFF AND THE EMFF IN THE LEADING TWIST

In order to carry out the RG summation, it is useful to expand the DA $\varphi_{\pi}^{(2)}(x,\mu^2)$ of leading twist 2, as well as the corresponding contribution to the em/transition amplitude over the conformal basis of the Gegenbauer harmonics ψ_n , where $\{\psi_n(x) = 6x\bar{x} C_n^{3/2}(x-\bar{x})\}$ and $b_n(\mu^2)$ are the coefficients of the conformal expansion,

$$\varphi_{\pi}^{(2)}(x,\mu^2) = \psi_0(x) + \sum_{n=2,4,\dots}^{\infty} b_n(\mu^2)\psi_n(x),$$
 (4a)

$$T_{\text{(tw2)}}(Q^2, \sigma; x) \otimes \varphi_{\pi}^{(2)}(x) = T_0(Q^2, \sigma) + \sum_{n=2,4,...}^{\infty} b_n(\mu^2) T_{(n)}(Q^2, \sigma; \mu^2).$$
 (4b)

Here, we follow the notations [3, 4] for the emFF, taking into account Eq.(2a): $Q^2 = -q^2$; $-(p-q)^2 = -s = \sigma \ge 0$. The similar notations for the transition FF: $-q_1^2 = Q^2$; $-q_2^2 = q^2 = \sigma \ge 0$ [5, 9]; for all Bjorken fractions the bar means $\bar{x} = 1 - x$, $\bar{u} = 1 - u$, . . .; the lower index n always numerates harmonics; $T_{(n)}$ is the projection of $T_{(tw2)}$ onto the ort ψ_n . The description of both these form factors are relatively close one to another from the point of view of a general frame: the initial correlators are similar to one another and differ by the replacement of π^0 with π^+ , the vector current with the axial current at one of the verties, they have practically the same diagrammatic presentations, and their corresponding LCSRs are also close. In particular, the virtuality of the "handbag" diagrams, $q(u) = \sigma u + Q^2 \bar{u}$, is the same for both amplitudes T, and the corresponding evolutional logarithm $L(u) = \ln(q(u)/\mu^2)$ is the same. For this reason, we will refer to the stages of calculation of the pion TFF that are already performed in [5, 9] and discuss the similar stages of calculations for the emFF.

We remove all the powers of ERBL evolution logarithms like $L \cdot (a_s V_0)$, $L \cdot (a_s^2 V_1)$,... that appear in further orders $a_s^k T^{(k)}$ of the amplitude in (3b), and collect them into the common exponential factor, see details in [9]. This procedure goes beyond the FOPT presented in the expansion (3b). The remaining non-logarithmic terms $\mathcal{H}^{(1)}$ of partial amplitudes $T_n^{(k)}$ ($T^{(0)} = H^{(0)}$) are accompanied by the evolution exponents for ψ_n -harmonics of DA expansion, the corresponding exponentials were presented in the general form in [5, 9–11]. Reducing the final result of the evolution to the one-loop level, we arrive at the compact expression on the right-hand side (rhs)

$$T_{(n)}(Q^2, \sigma; \mu^2) \stackrel{\text{1-loop}}{\longrightarrow} H_{(n)}^{(1)} = H^{(0)}(u) \underset{u}{\otimes} \left[\mathbb{1} + \bar{a}_s(u) \mathcal{H}^{(1)}(u, v) \right] \left(\frac{\bar{a}_s(u)}{a_s(\mu^2)} \right)^{\nu_n} \underset{v}{\otimes} \psi_n(v) , \tag{5}$$

where the notation for the running coupling $\bar{a}_s = \bar{\alpha}_s/(4\pi)$, $\bar{a}_s(u) = \bar{a}_s(q(u)) \equiv \bar{a}_s(\sigma u + Q^2\bar{u})$ is used; $H^{(0)}(u)$ is the Born term of the perturbative expansion, $\mathcal{H}^{(1)}(u,v)$ is the next-to-leading-order (NLO) coefficient function; the index n means the number of the harmonic ψ_n . This expression coincides in structure with the corresponding RG-summed expression for the TFF [5, 9, 10], differing from the latter by the forms of the amplitudes $H^{(0)}(u)$, $\mathcal{H}^{(1)}(u,v)$ in comparison with the ones $T_0(u)$, $\mathcal{T}^{(1)}(u,v)$ there. The quantities entering into (5) are the following (for $\mathcal{H}^{(1)}$ we refer to Appendix A):

$$H^{(0)}(u) \equiv H^{(0)}(Q^2, \sigma; u) = \frac{u}{\sigma u + Q^2 \bar{u}};$$
 (6a)

$$1 \equiv \delta(v - u); \tag{6b}$$

$$V_0(u,v) \underset{v}{\otimes} \psi_n(v) = -\frac{1}{2} \gamma_0(n) \psi_n(u); \nu_n = \frac{1}{2} \frac{\gamma_0(n)}{\beta_0}.$$
 (6c)

Here the ERBL kernel $V_0(y, z)$ is explicitly defined in Eq. (A2a), $a_s\gamma_0(n)$ denotes the one-loop anomalous dimension of the corresponding composite operator of the leading twist and β_0 is the first coefficient of the QCD β -function,

both defined in (A4). Note, that the running coupling $\bar{a}_s^{\nu}(u)$ and the coefficient functions $H^{(0)}(u)$, $\mathcal{H}^{(1)}(u,v)$ do not enter into (5) as a simple product, but as their convolution. It is important to note that for the case of ψ_0 harmonic, the results of RG summation in $H_{(0)}^{(1)}$ do not manifest themself due to the conservation of the vector (axial) current, $\gamma_0(n=0)=0, \nu_{n=0}=0$ in Eqs.(5), (6c),

$$H_{(0)}^{(1)} = H^{(0)}(u) \underset{u}{\otimes} \left[\mathbb{1} + \bar{a}_s(u) \mathcal{H}^{(1)}(u, v) \right] \underset{v}{\otimes} \psi_0(v) . \tag{7}$$

This circumstance may serve as a test for the current results.

For small values of σ , this convolution has only a formal rather than a physical meaning, even at large Q^2 . This becomes obvious when the scale argument $\sigma u + Q^2 \bar{u}$ approaches small values for $u \to 1$, even if Q^2 is large, so the perturbative expansion becomes unprotected. This problem is avoided when the amplitude $H_{(n)}^{(1)}$ is involved in the dispersion relation in LCSR. As we show below, in this case, an equation like Eq. (5) can still be safely used in the emFF calculation even for small Q^2 .

III. DISPERSION RELATION IN CONNECTION WITH THE RG TECHNIQUE, THE TWIST-2

A. Dispersion relation for the amplitude

As we now demonstrate, summing over all radiative corrections in Eq. (5) entails a new contribution to the imaginary part of the amplitude $H_{(n)}(Q^2, -\sigma)$ and generates a new spectral density $\rho_n^{\text{tw}2}$, where σ is dual to s. This contribution marks an important difference from the standard version of the LCSRs [2, 14–16]. To be more specific, the imaginary part of the Born contribution is induced by the singularity of $H_0(Q^2, -\sigma; u)$ multiplied by a power of the logarithms that originated from the truncated pQCD series (usually a few terms) of radiative corrections. In contrast, the RG summed radiative corrections lead to a term in the spectral density $\rho_n^{\text{tw}2}$ that originates from the $\mathbf{Im}_{s'}\left[\bar{a}_s^{\nu}(Q^2\bar{u}-s'u)\right]/\pi$ contribution in the rhs of Eq.(5),

$$\rho_n^{\text{tw}2}(s', Q^2) = \mathbf{Re}\left[\frac{u}{(Q^2\bar{u} - s'u)}\right] \frac{\mathbf{Im}_{s'}[\bar{a}_s^{\nu}(Q^2\bar{u} - s'u)]}{\pi \, a_s^{\nu}(\mu_0^2)} \otimes \psi_n(u) + \mathbf{0}. \tag{8a}$$

The symbol $\mathbf{0}$ in the rhs of (8a) means the trace of the previous "standard" [3, 4, 6] contribution that is now proportional to $\frac{1}{\pi}\mathbf{Im}(H_0)\mathbf{Re}[\bar{a}_s^{\nu}]=0$ because the pole of the first multiplier at $Q^2\bar{u}-s'u=0$ coincides with the argument of the second one; at the same time, one should put $\bar{a}_s^{\nu}(0)=0$ formally. Let us introduce an auxiliary quantity J_n to deal with the dispersion integral of expression (5),

$$J_n(Q^2, \sigma) = \int_0^{s_0} \frac{ds'}{s' + \sigma} \, \rho_n^{\text{tw}2}(s', Q^2) \,. \tag{8b}$$

Note that the finite upper limit s_0 in the integral (8b) is the interval of duality [3, 4, 6], while the integral by itself appears due to the "subtraction of continuum" inherent in the LCSR. Replacing the integration variable s', $s' \to s = s'u - Q^2\bar{u}$ in (8b) and taking into account that the integral exists only for $s \ge 0$, one obtains

$$J_n(Q^2, \sigma) = \frac{1}{a_s^{\nu_n}(\mu_0^2)} \left(\int_0^{s(u)} \frac{ds}{s} \frac{-u}{(s+q(\bar{u}))} \cdot \frac{1}{\pi} \mathbf{Im}[\bar{a}_s^{\nu_n}(-s-i\varepsilon)] \right) \otimes (\theta(u \geqslant u_0)\psi_n(u)), \quad (9a)$$

where the upper limit
$$s(u) = (Q^2 + s_0)(u - u_0) \ge 0$$
, $u_0 = Q^2/(Q^2 + s_0)$; $q(u) = \sigma u + Q^2 \bar{u}$. (9b)

In the rhs of (9a), there appears the spectral density ρ_{ν} for \bar{a}_{s}^{ν} ,

$$\rho_{\nu}(s) = \frac{1}{\pi} \mathbf{Im} [\bar{a}_{s}^{\nu}(-s - i\varepsilon)], \qquad (10a)$$

which is the key quantity of FAPT, see also its expression in Eq.(B3) in Appendix B. After a simple algebra with the dispersion integral in the parentheses in (9a) and taking into account the definitions of FAPT couplings $\mathcal{A}_{\nu}, \mathcal{I}_{\nu}$ in

Eq.(B4) and (B6) respectively, one arrives at the expression

$$\frac{1}{x} \left(\int_0^y = \int_0^\infty ds - \int_y^\infty ds \right) \left(\frac{1}{s+x} - \frac{1}{s} \right) \rho_{\nu}(s) = \frac{1}{x} \left[\left(\mathcal{A}_{\nu}(x) - \mathcal{A}_{\nu}(0) \right) - \left(\mathcal{I}_{\nu}(y, x) - \mathcal{I}_{\nu}(y, 0) \right) \right]. \tag{10b}$$

Hereinafter we use the notation x = q(u) and y = s(u) for brevity. Substituting (10b) in (9a), we arrive at the final expression for J_n ,

$$J_{n}(Q^{2},\sigma) = \frac{u}{x} \frac{1}{a_{s}^{\nu_{n}}(\mu_{0}^{2})} \left[\mathcal{A}_{\nu_{n}}(x) - \mathcal{A}_{\nu_{n}}(0) - \left(\mathcal{I}_{\nu_{n}}(y,x) - \mathcal{I}_{\nu_{n}}(y,0) \right) \right] \Big|_{\substack{x=q(u)\\y=s(u)}} \otimes \left(\theta(u \geqslant u_{0}) \psi_{n}(u) \right), \tag{11}$$

where we find the result of the dispersion relation with one subtraction. Further, we set $\mathcal{A}_{\nu}(0) = \mathfrak{A}_{\nu}(0) = 0$ at $0 < \nu \le 1$ following our necessary requirement that was justified in [9, 11] for any model of the FAPT coupling constant at the zero value of its argument. Here we obtained an effective coupling constant in square brackets in (11) that can be rewritten as

$$\Delta_{\nu}(y,x) = \mathcal{I}_{\nu}(0,x) - \mathcal{I}_{\nu}(y,x) + \mathcal{I}_{\nu}(y,0) = \mathcal{A}_{\nu}(x) - \mathcal{I}_{\nu}(y,x) + \mathfrak{A}_{\nu}(y), \tag{12}$$

where the generalized charge $\mathcal{I}_{\nu}(y,x)$ reduces to $\mathcal{I}_{\nu}(0,x) = \mathcal{A}_{\nu}(x)$, $\mathcal{I}_{\nu}(y,0) = \mathfrak{A}_{\nu}(y)$, see Eq.(B7). This cumbersome tree-term construction of Δ_{ν} in (12) is due to the "subtraction" inherent in the LCSR. Indeed, at $s_0, y \to \infty$ the effective charge Δ_{ν} tends $\mathcal{A}_{\nu}(x)$, *i.e.*, tends to the spacelike FAPT coupling constant only, as is expected.

The particular $H_{(n)}^{(2)}$ in (5) is transformed within the dispersion approach and with the help of Eq.(11,12) to

$$H_{(n)}^{(1)LCSR} = \frac{1}{a_s^{\nu_n}(\mu_0^2)} H_0(u) \left\{ \Delta_{\nu_n}(s(u), q(u)) \otimes \mathbb{1} + \Delta_{(1+\nu_n)}(s(u), q(u)) \otimes \mathcal{H}^{(1)}(u, v) \right\} \otimes (\theta(v \geqslant v_0) \psi_n(v)), \quad (13)$$

here the effective coupling constants Δ_{ν} replaces the initial QCD coupling constant \bar{a}_{s}^{ν} in RG-summed Eq.(5). So, the final result of the LCSR (twist 2) can be obtained by employing a linear combination of generalized FAPT couplings \mathcal{I}_{ν} collected into a single effective Δ_{ν} . For the important partial case of asymptotic DA ψ_{0} , at $n=0, \nu_{n=0}=0$, this effective coupling Δ_{ν} turns into

$$\Delta_0(y, x) = A_0(x) - \mathcal{I}_0(y, x) + \mathfrak{A}_0(y) \to 1; \ \Delta_1(y, x) = A_1(x) - \mathcal{I}_1(y, x) + \mathfrak{A}_1(y), \tag{14a}$$

and $\mathcal{A}_1(x), \mathfrak{A}_1(y)$ are expressed in terms of elementary functions [13], see (B1) in Appendix B. Finally, for the contribution of ψ_0 -harmonics to $H^{(2)LCSR}$ we obtain

$$H_{(0)}^{(1)LCSR} = H^{(0)}(u) \underset{u}{\otimes} \left\{ \mathbb{1} + \Delta_1(s(u), q(u)) \mathcal{H}^{(1)}(u, v) \right\} \underset{v}{\otimes} (\theta(v \geqslant v_0) \psi_0(v)). \tag{14b}$$

It should be compared with Eq.(7) that was obtained at the same condition before the dispersion relation is used: the single change is the replacement of the standard $\bar{a}_s(u)$ with the new coupling $\Delta_1(s(u), q(u))$ in Eq.(14b). Concluding, one can present the chain of all the previous transformations with coupling constants as

FOPT RG resum, Eq.(5): LCSR for
$$F_{\pi}$$
, Eq.(12): dispersion relat. + Only dispersion relat.
duality model with $s_0 \to \infty$ $a_s^n(\mu^2) \longrightarrow \bar{a}_s^{\nu}(x = \sigma u + Q^2\bar{u}) \longrightarrow \Delta_{\nu}(y, x) \Longrightarrow \mathcal{A}_{\nu}(x = \sigma u + Q^2\bar{u})$.

B. Contribution of the Borel image to the LCSR

The application of the Borel transformation $M^2\hat{\mathbf{B}}_{(\sigma\to\mathbf{M}^2)}$ to the amplitude $H_{(n)}^{(1)\text{LCSR}}$ to obtain the complete contribution $F_{\pi}^{(1)\text{LCSR}}$ to the LCSR destroys the universality of the coupling $\mathcal{I}_{\nu}(y,x)$, which is manifested in Eqs.(13,14b),

creating a variety of forms of the FAPT coupling constants. So, applying $M^2\hat{\mathbf{B}}_{(\sigma\to\mathbf{M}^2)}$ to $H^{(0)}(u)\Delta_{\nu}(s(u),q(u))$ and using (C4b), (10a) and (B6), one arrives at

$$F_{\pi,n}^{(1)\text{LCSR}}(Q^2, M^2) = M^2 \hat{\mathbf{B}} H_{(n)}^{(1)\text{LCSR}} = \frac{1}{a_s^{\nu_n}(\mu_0^2)} \left\{ \left[\mathfrak{A}_{\nu_n}(s(u)) + \int_0^{s(u)} \rho_{\nu_n}(s) \omega_1(s, u) ds \right] \underset{u}{\otimes} \mathbb{1} + \left[\mathfrak{A}_{(\nu_n+1)}(s(u)) + \int_0^{s(u)} \rho_{(\nu_n+1)}(s) \omega_1(s, u) ds \right] \underset{u}{\otimes} \mathcal{H}^{(1)}(u, v) \right\} \exp\left(-\frac{Q^2}{M^2} \frac{\bar{u}}{u} \right) \underset{v}{\otimes} (\theta(v \geqslant v_0) \psi_n(v))$$
(15a)

where the weight $\omega_1(s, u) = \frac{1}{s} \left[1 - \exp\left(-\frac{s}{M^2 u}\right) \right]$, $v_0 = u_0$. Equation (15a) provides the contribution of twist-2 for pion's emFF in the framework of the LCSR at RG summation at LO. Taking into account that $\mathcal{I}_{\nu}(s(u),0) = \mathfrak{A}_{\nu}(s(u))\Big|_{\nu\to 0} = 1$ for the first term, and $\rho_{(\nu)}\Big|_{\nu\to 0} \to 0$ for the second one in square brackets, one arrives at the representation of Eq. (15a) at different n,

$$F_{\pi,0}^{(1)\text{LCSR,LO}}(Q^2, M^2) = \int_{u_0}^{1} \exp\left(-\frac{Q^2}{M^2} \frac{\bar{u}}{u}\right) \psi_0(u) du, (n=0); \tag{16a}$$

$$F_{\pi,n>0}^{(1)\text{LCSR,LO}}(Q^2, M^2) = \frac{1}{a_s^{\nu_n}(\mu_0^2)} \left[\mathfrak{A}_{\nu_n}(s(u)) + \int_0^{s(u)} \rho_{\nu_n}(s) \omega_1(s, u) \, ds \right] \exp\left(-\frac{Q^2}{M^2} \frac{\bar{u}}{u} \right) \underbrace{\otimes}_u \left(\theta(u \geqslant u_0) \psi_n(u) \right), \quad (16b)$$

where the ψ_0 -projection in the first line, Eq.(16a), coincides with the standard FOPT [3, 4, 6] result due to the conservation of the vector current. The expressions for higher harmonics contain the results of RG-summation within the square brackets in the second line, Eq. (16b), while the complete Eq. (15) provides the NLO contribution in addition to Eq.(16b).

CONTRIBUTIONS OF HIGHER TWISTS 4,6 TO THE LCSR

Twist-4 contribution via the dispersion relation

As was mentioned above, the twist-4 contribution is crucial for improving precision at moderate Q^2 . This contribution becomes comparable with the twist-2 one at small $Q^2 \sim 0.5 \,\mathrm{GeV}^2$ see the discussion in [4]. The amplitude corresponding to this contribution reads [4]

$$T_{(\text{tw}4)}(Q^2, -s) = \left(\frac{1}{\bar{u} Q^2 - u s}\right)^2 \delta_{\text{tw}-4}^2(\mu^2) \otimes (u \varphi_{\pi}^{(4)}(u));$$
(17a)

$$\delta_{\text{tw-4}}^{2}(\mu^{2}) = \left[\frac{a_{s}(\mu^{2})}{a_{s}(\mu_{0}^{2})}\right]^{\nu_{t4}} \delta_{\text{tw-4}}^{2}(\mu_{0}^{2}), \nu_{t4} = \gamma_{t4}/\beta_{0}, \gamma_{t4} = C_{F} 8/3, \nu_{t4} = C_{F} 8/(3\beta_{0}) < 1;$$
 (17b)

$$\delta_{\text{tw-4}}^2(\mu_0^2) = 0.21 \text{ GeV}^2, \varphi_{\pi}^{(4)}(u) = \frac{20}{3} u \bar{u} \left(1 - u(7 - 8u) \right). \tag{17c}$$

The spectral density $\rho^{\text{tw}4}$ taken on the variable s for the amplitude (17a) is determined by the imaginary part that appears only due to the first factor there. Thus $\rho^{\text{tw}4}(s)$ is proportional to $\left[\delta(\bar{u}/u\,Q^2-s)\right]_s'$, which leads to the known expression [4] that is also derived in Appendix D.

Here we utilize an opposite approach, suggesting that the scale μ^2 of two-particle DA of twist 4 is equal to quark virtuality $\bar{u}\,Q^2-u\,s=\mu^2,\,i.e.$, $\delta_{\rm tw-4}^2(\bar{u}\,Q^2-u\,s\to\mu^2)$ in the l.h.s. of (17b). This natural suggestion means the same dependence of the running coupling $\bar{a}_s^{\nu}(\bar{u}\,Q^2-u\,s)$, which in turn, leads to inclusion latter into the dispersion relation (for the amplitude) that completely changes spectral density $\rho^{\text{tw4}}(s')$ that is similar to the consideration in Sec. III. In other words, a composition of RG running together with the dispersion relation for the twist 4 leads to a nonpower series and the appearance of coupling constants like FAPT in full analogy with the results in the leading twist 2. Following the procedure used in Sec. III (elaborated in [5, 9–11]), see Eq.(8) there, one obtains

$$\rho^{\text{tw4}}(s', Q^2) = \mathbf{Re} \left[\frac{1}{(Q^2 \bar{u} - s' u)^2} \right] \frac{1}{\pi} \mathbf{Im} [\bar{a}_s^{\nu_{t4}} (Q^2 \bar{u} - s' u)] \otimes \left(u \varphi_{\pi}^{(4)}(u) \right) + \mathbf{0},$$
 (18a)

$$H_{\text{(tw4)}}^{\text{LCSR}}(Q^2, \sigma) = \frac{\delta_{\text{tw-4}}^2(\mu_0^2)}{a_s^{\nu_{t4}}(\mu_0^2)} \int_0^{s_0} \frac{ds'}{s' + \sigma} \rho^{\text{tw4}}(s', Q^2), \tag{18b}$$

where $\sigma = -s \geqslant 0$. The symbol $\bf 0$ in the rhs of (18a) means the trace of the previous FOPT contribution that is now proportional to $\frac{1}{\pi} {\bf Im} \left(H_0^2 \right) {\bf Re}[\bar{a}_s^{\nu}] = 0$, like for the case of twist 2. Replacing the integration variable $s', \ s' \to s = s'u - Q^2\bar{u}$ in (18b) and taking into account that the dispersion integral exists only for $s \geqslant 0$, one obtains

$$H_{\text{(tw4)}}^{\text{LCSR}}(Q^2, \sigma) = \frac{\delta_{\text{tw-4}}^2(\mu_0^2)}{a_s^{\nu}(\mu_0^2)} \left(\int_0^{s(u)} \frac{ds}{s^2} \frac{1}{(s+q(\bar{u}))} \frac{1}{\pi} \mathbf{Im}[\bar{a}_s^{\nu}(-s-i\varepsilon)] \right) \otimes \left(u \,\theta(u \geqslant u_0) \varphi_{\pi}^{(4)}(u) \right), \tag{19}$$

where the upper limit $s(u) = (s_0 + Q^2)(u - u_0)$; $s_0 \ge s(u) \ge 0$; $u_0 = Q^2/(Q^2 + s_0)$; $q(u) = \sigma u + Q^2 \bar{u}$. Performing a simple algebra with the dispersion integral in the first parentheses in (19) and using (10a), one arrives at the expression

$$\frac{1}{x^2} \left(\int_0^\infty ds - \int_y^\infty ds \right) \left(\frac{1}{s+x} - \frac{1}{s} + \frac{x}{s^2} \right) \rho_{\nu}(s) =
\frac{1}{x^2} \left[\mathcal{A}_{\nu}(x) - \mathcal{A}_{\nu}(0) - x \mathcal{A}'_{\nu}(0) \right] - \frac{1}{x^2} \left[\mathcal{I}_{\nu}(y,x) - \mathcal{I}_{\nu}(y,0) - x \mathcal{I}'_{\nu}(y,0) \right] ,$$
(20)

where $\mathcal{I}'_{\nu}(y,0) \equiv \frac{d}{dx}\mathcal{I}_{\nu}(y,x)\Big|_{x=0}$ means the differentiation by the second argument (recall that x=q(u), y=s(u)). In Eq.(20) for twist 4 we get the dispersion relation with two subtractions in contrast to twist 2 result with a single subtruction in (11). Substituting Eq.(20) in Eq.(19), one obtains the final result for $H_{\text{(tw4)}}^{\text{LCSR}}$,

$$H_{\text{(tw4)}}^{\text{LCSR}}(Q^{2}, \sigma) = \frac{\delta_{\text{tw-4}}^{2}(\mu_{0}^{2})}{x^{2}} \frac{1}{a_{s}^{\nu_{t4}}(\mu_{0}^{2})} \left[\mathcal{A}_{\nu_{t4}}(x) - \mathcal{A}_{\nu_{t4}}(0) - x \mathcal{A}'_{\nu_{t4}}(0) - \left(\mathcal{I}_{\nu_{t4}}(y, x) - \mathcal{I}_{\nu_{t4}}(y, 0) - x \mathcal{I}'_{\nu_{t4}}(y, 0) \right) \right] \Big|_{\substack{x=q(u) \\ v=s(u)}} \otimes \left(u\theta(u \geqslant u_{0})\varphi_{\pi}^{(4)}(u) \right).$$

$$(21)$$

Following our necessary condition [9] for the values of the FAPT couplings at zero argument, wherever the FAPT ("minimal") couplings are ill-defined we extend our constraints [11] up to the first derivative $\mathcal{A}_{\nu}(0) = \mathcal{A}'_{\nu}(0) = 0$ at zero. Taking into account this condition and applying the Borel transform to $H_{(\text{tw}4)}^{\text{LCSR}}$ in (21), one obtains the contribution for $F_{\pi}^{(\text{tw}4)}$,

$$F_{\pi}^{(\text{tw4})}(Q^{2}, M^{2}) = M^{2} \hat{\mathbf{B}}_{(\sigma \to \mathbf{M}^{2})} H_{(\text{tw4})}^{\text{LCSR}}(Q^{2}, \sigma), \text{ where}$$

$$H_{(\text{tw4})}^{\text{LCSR}}(Q^{2}, \sigma) = \frac{\delta_{\text{tw-4}}^{2}(\mu_{0}^{2})}{x^{2}} \left\{ \frac{1}{a_{s}^{\nu_{t4}}(\mu_{0}^{2})} \left[\mathcal{A}_{\nu_{t4}}(x) - \mathcal{I}_{\nu_{t4}}(y, x) + \mathfrak{A}_{\nu_{t4}}(y) + x \mathcal{I}'_{\nu_{t4}}(y, 0) \right] \right\} \otimes \left(u\theta(u \geqslant u_{0})\varphi_{\pi}^{(4)}(u) \right). \tag{22}$$

We conclude that the amplitude $H_{(\text{tw}4)}^{\text{LCSR}}$ can be expressed in terms of an effective coupling (in square brackets) that consists of generalized FAPT couplings \mathcal{I}_{ν} and its derivatives (similarly to the corresponding case of TFF [5, 9, 11]). Again, if the single parameter of the LCSR s_0 tends to ∞ , then the effective coupling tends to the spacelike $\mathcal{A}_{\nu_{t4}}(x)$.

The subsequent Borel transform changes this correspondence, creating new constructions. Indeed, applying Eq. (C3)

The subsequent Borel transform changes this correspondence, creating new constructions. Indeed, applying Eq.(C3) to the last two terms in (22), and Eq.(C4) to the first difference $(\mathcal{A}_{\nu}(x) - \mathcal{I}_{\nu}(y,x))/x^2$, we arrive at

$$F_{\pi}^{(\text{tw4})\text{LCSR}}(Q^{2}, M^{2}) = \frac{\delta_{\text{tw-4}}^{2}(\mu_{0}^{2})}{a_{s}^{\nu_{t4}}(\mu_{0}^{2})} \cdot \left[\mathfrak{A}_{\nu_{t4}}(s(u)) + \frac{1}{M^{2}u} \mathcal{I}'_{\nu_{t4}}(s(u), 0) + \int_{0}^{s(u)} \rho_{\nu_{t4}}(s)\omega_{2}(s, u)ds \right] \exp\left(-\frac{Q^{2}}{M^{2}} \frac{\bar{u}}{u}\right) \otimes (\theta(u \geqslant u_{0})\varphi_{\pi}^{(4)}(u)),$$

$$(23)$$

where the weight $\omega_2(s,u) = \frac{1}{s^2} \left[\exp\left(-\frac{s}{M^2 u}\right) - \left(1 - \frac{s}{M^2 u}\right) \right]$ contains two subtractions of the expansion of the exponential. The integration of the second term $\sim \mathcal{I}_{\nu}'$ in (23) can be performed with the help of Eqs.(B10, B11, B12) in Appendix B.

The RG (summed) result in (23) should be compared with the initial unsummed expression for $F_{\pi}^{(tw4)}(Q^2, M^2)$ (or one that is presented in (D4)),

$$F_{\pi}^{(4)}(Q^2, M^2) = \delta_{\text{tw-4}}^2(\mu^2) \cdot \left[\delta(u - u_0) \frac{u}{Q^2} + \frac{1}{M^2 u} \right] \exp\left(-\frac{Q^2}{M^2} \frac{\bar{u}}{u} \right) \otimes \left(\theta(u \geqslant u_0) \varphi_{\pi}^{(4)}(u) \right). \tag{24}$$

Here the authors of [3, 4, 6] used an ad hoc ansatz for the normalization scale $\mu^2 \to \mu_u^2 = M^2 u + Q^2 \bar{u}$; see the discussion of it in Appendix C. The comparison of both results for twist-4 are presented in Fig.2, where for $\delta_{\text{tw-4}}^2(\mu_0^2)$ in Eq.(23), we used the numerical estimate based on the relation of the latter with the parameter $\lambda_q^2/2$ of nonlocal condensate (NLC) [17]; see the beginning of Sec.V A. This parameter simultaneously determines the features of the twist-2 pion DA in the framework of the NLC QCD SR [18, 19]. So, the twist-2 and twist-4 contributions of are mutually related by means of the influence on $\varphi_{\pi}^{(2)}(x,\mu^2)$, its Gegenbauer expansion coefficients $\{b_n(\mu_0^2)\}$ in Eq.(4), and the coefficient $\delta_{\text{tw-4}}^2(\mu_0^2)$. Note the important role of condensate nonlocality was shown in the calculation of emFF within QCD sum rules in [20].

As is seen in Fig. 2, the result of $F_{\pi}^{(\text{tw4})\text{LCSR}}$ in Eq.(23) is almost everywhere expectedly lower than the standard $F_{\pi}^{(4)}$ in Eq.(24). The behavior with Q^2 for both cases is close to each other, although the origins of the corresponding

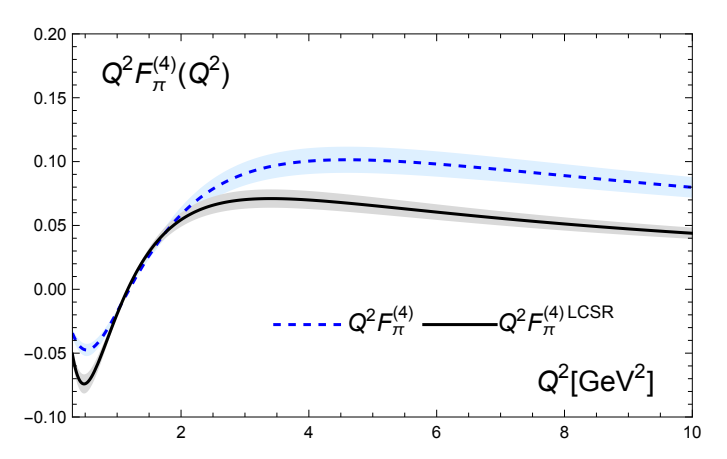


FIG. 2: Solid (black) line is the result of RG sum $F_{\pi}^{(4)LCSR}$ in Eq.(23); the dashed (blue) line is the standard result $F_{\pi}^{(4)}$ in Eq.(24) with the value of $\delta_{tw-4}^2(\mu_0^2)$ in [4], both curves are taken at $M^2 = 1.2 \,\text{GeV}^2$.

spectral densities are different. Moreover, $F_{\pi}^{(\text{tw4})\text{LCSR}}$ is well founded at small $Q^2 < 1 \text{ GeV}^2$ from the view point of radiative corrections. Nevertheless, one should not fall below the scale $Q_{thr}^2 \approx 0.4 - 0.5 \text{ GeV}^2$ – the minimum of $Q^2 F^{(\text{tw4})\text{LCSR}}(Q^2)$ for another reason; starting with this scale, the twist hierarchy becomes violated.

B. Twist-6 contribution

The factorizable twist-6 contribution [3] is

$$F_{\pi}^{(\text{tw6})}(Q^2) = \frac{4\pi C_F}{3f_{\pi}^2 Q^4} \, \delta_{\text{tw-6}}^2(\mu_0^2) \,, \qquad \text{where}$$
 (25)

$$\delta_{\text{tw-6}}^{2}(\mu_{0}^{2} = 1 \,\text{GeV}^{2}) = \langle \sqrt{\alpha_{s}} \bar{q} q \rangle^{2} = (1.61 \pm 2 \cdot 0.26) \times 10^{-4} \,\text{GeV}^{6} - \text{ "the best fit" in [5]}$$
 (26)
$$\langle \sqrt{\alpha_{s}} \bar{q} q \rangle^{2} = (1.84^{+0.84}_{-0.24}) \times 10^{-4} \,\text{GeV}^{6} \,[6] \,,$$

Further, we will use our best-fit estimate ¹ in Eq.(26), which overlaps within errors with values given in [6].

V. NUMERICAL ESTIMATES OF F_{π} IN DIFFERENT LCSR APPROACHES

Firstly, we discuss in detail the status of nonperturbative inputs of different twists that significantly affect the resulting estimates of F_{π} within the LCSRs. Then, in the next subsections, we will consider our predictions for F_{π} at different approximations in comparison with experimental data.

A. Nonperturbative inputs of the LCSR

In items (**i** - **iv**) below, we discuss the admissible models of the DA of twist-2 and the factors at twists-4 and -6 that are compatible with the results of lattice calculation [21] and the phenomenological analysis of experimental data on TFF in [5]. Further, for duality interval s_0 of the LCSR we admit, the estimate $s_0 = 0.7 \,\text{GeV}^2$ [3, 4, 6].

(i) We will use the corrected domain of the Gegenbauer expansion coefficients for the pion DA $\varphi_{\pi}^{(2)}(x, \mu_0^2 = 1 \text{GeV}^2)$ – $(b_2^{\text{BMS}}(\mu_0^2) = \mathbf{0.159}_{-0.027}^{+0.025}, b_4^{\text{BMS}}(\mu_0^2) = -\mathbf{0.098}_{-0.03}^{+0.05})$. Such modified BMS (BMSmod) model $\varphi_{\pi}^{(2)\text{BMS}}$ represents a compromise of QCD SR [19, 22] results, lattice simulation results [21], and phenomenological analysis of the pion TFF [5], see Fig.1 there, which are reproduced as Fig. 6 in Appendix E. The vertices of the rectangle that bounds the uncertainty domain (b_2, b_4) are:

$$\{(b_2 = 0.132, b_4 = -0.06), (b_2 = 0.185, b_4 = -0.08), (b_2 = 0.185, b_4 = -0.16), (b_2 = 0.132, b_4 = -0.12)\}.$$

The different lattice estimates [21] read $b_2(\mu_L^2) = 0.116 \pm 0.020$ (N³LO) at $\mu_L^2 = (2 \text{ GeV})^2$, which just coincide with the BMSmod component $b_2^{\text{BMS}}(\mu_0^2) = \mathbf{0.159}$ in [5] and agrees with other lattice estimates $(b_2(\mu_L^2) = 0.131 \pm 0.041, b_4(\mu_L^2) = -0.39 \pm 0.76)$ presented in [23].

- (ii) The estimate of the twist-4 parameter $\delta_{\text{tw-4}}^2(\mu_0^2 = 1 \,\text{GeV}^2) \approx \lambda_q^2/(2 \cdot 1.075)$ which is used here, is taken from QCD SR in [17]. The estimate of the "nonlocality parameter" λ_q^2 [24, 25] is $\lambda_q^2 \in [0.4-0.45] \,\text{GeV}^2$ [5], that leads to $\delta_{\text{tw-4}}^2 = \mathbf{0.198} \pm \mathbf{0.01} \pm \mathbf{0.01} \,\text{GeV}^2$ (where the first uncertainty is due to variation of λ_q^2 and the second one to the analysis of QCD SR [17] for $\delta_{\text{tw-4}}^2$), while the previous estimates were $\delta_{\text{tw-4}}^2(\mu_0^2) = 0.17, 0.18 \,\text{GeV}^2$ that correspond to [4], [6] respectively.
- (iii) An alternative to the BMSmod DA is the so-called "platykurtic" DA [26] $(b_2^{pk}=0.081,b_4^{pk}=-0.019)$ that corresponds to the highest estimate of $\lambda_q^2=0.45\,\mathrm{GeV^2}$, see Fig.6 that leads to $\delta_{\mathrm{tw-4}}^2=0.209\pm0.01\pm0.01\,\mathrm{GeV^2}$ [5].
- (iv) The value of the scale parameter for tw-6 in Eq.(25) is taken from the results [5] $\langle \sqrt{\alpha_s} \bar{q}q \rangle^2 = (\mathbf{1.61} \pm \mathbf{2} \cdot \mathbf{0.26}) \times 10^{-4} \,\text{GeV}^6$ that is in mutual relation with the pair $(b_2^{\text{BMS}}, b_4^{\text{BMS}})$, while the best fit of data processing in [5] with $\chi_{\text{ndf}}^2 \simeq 0.4$ provides $(b_2^{bf}(\mu_0^2) = \mathbf{0.112}, b_4^{bf}(\mu_0^2) = -\mathbf{0.029})$ for DA^{bf}.

Note that both the BMSmod, see item (i), and the platykurtic DA in item (iii) are included in the 1σ level of the best-fit point DA^{bf} in item (iv), see Fig. 6. The modern lattice results for the profile of the pion DA in [27] demonstrate the same behavior as the mentioned DA^{bf} within $0.2 \le x \le 0.8$, see the corresponding profiles in Fig.7.

Summarizing, we will use those of nonperturbative inputs (i-ii,iv) that have already provided a good agreement at the 1σ level between the experimental data of the process $\gamma + \gamma^* \to \pi^0$ and the corresponding predictions obtained within the theoretical framework of [5] (see Fig.1 there) and [11].

B. "Hybrid" approach and preliminary comparisons

Here we consider the results for the components of the emFF: $F_{\pi}^{(\text{tw2})\text{LCSR},\text{LO}}$ – for the leading twist-2 in Eq.(16) obtained within the LCSR with RG summation that are taken for the BMSmod DA [5]; $F_{\pi}^{(\text{tw4})\text{LCSR}}$ – for twist-4

¹ we recognize now that the conservative uncertainty should be approximately twice as large as that mentioned in [5]

in Eq.(23) obtained at the same condition; $F_{\pi}^{(\text{tw6})}$ – for the twist-6 in Eq.(25). The curves for all the components are presented in Fig.3 for comparison. It is seen that the hierarchy of twist contributions is disturbed around small

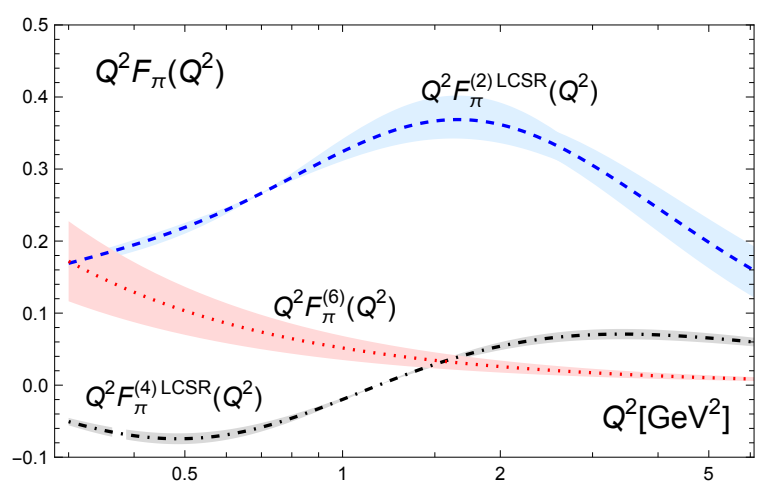


FIG. 3: Different twist contributions of the LO RG summation: the upper widening, blue strip is twist-2 $F_{\pi}^{(\text{tw}2)\text{LCSR},\text{LO}}$; the thin, dashed-dotted grey line is twist-4 $F_{\pi}^{(\text{tw}4)\text{LCSR}}$; the red narrowing strip with dots is twist-6 $F_{\pi}^{(\text{tw}6)}$.

 $Q_{\rm thr}^2 \approx 0.4 \, {\rm GeV^2}$.

Collected together, these components constitute the self-consistent and completed result F_{π}^{LCSR} ,

$$F_{\pi}^{\text{LCSR}}(Q^2) = F_{\pi}^{(\text{tw2})\text{LCSR,LO}}(Q^2) + F_{\pi}^{(\text{tw4})\text{LCSR}}(Q^2) + F_{\pi}^{(\text{tw6})}(Q^2). \tag{27}$$

This F_{π}^{LCSR} is valuable and can be compared with the experimental data independently, which are presented in Fig.4. There, we use the DA^{bf} for the twist-2 in the left panel and the BMSmod DA in the right one at the parameters twist-4

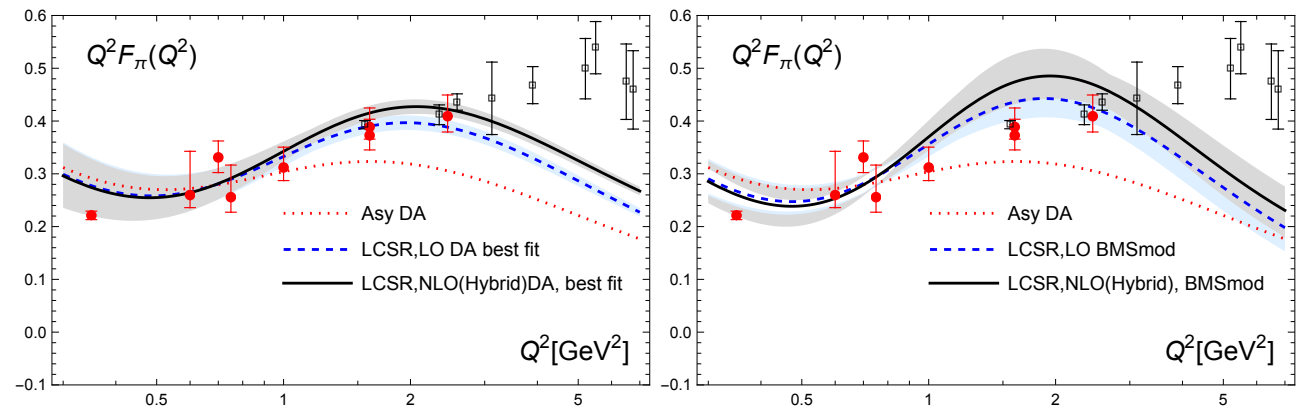


FIG. 4: Predictions for LO LCSR, F_{π}^{LCSR} in Eq.(27) for DA^{bf}, for the bunch of BMSmod, and for Asy DAs are presented with dotted red line, blue and grey strips - uncertainties in LO and NLO respectively in both panels. The red discs with error bars are the experimental data from [7]; the open boxes with bars are the recent lattice predictions [28]. **Left:**Dashed blue line, and in addition to them the standard NLO LCSR [4] corrections – upper solid black line (named hybrid) are based on DA^{bf} from item (iv). **Right:** The same curve designations for F_{π}^{LCSR} and NLO LCSR corrections based on the bunch of BMSmod DAs.

and twist-6 from items (ii) and (iv) respectively. The upper solid curves in both panels show "hybrid" estimates, for which F_{π}^{LCSR} in Eq.(27) (dashed lines) are supplemented with the NLO corrections taken within FOPT from [4]. Of course, these "hybrid" results appear at the mechanistic addition of NLO FOPT corrections to the base that was summed by RG, i.e., they are the components of substantially different species. Considering that the FOPT terms are always larger than the FAPT ones, the upper solid curves can be considered *only as an upper bound* for the emFF.

One can conclude that both the pion DA models DA^{bf} and bunch of BMSmod DA [5] (see Appendix E) used sufficiently well describe the experimental data on F_{π} [7], if one takes into account inherent uncertainties of nonper-

turbative inputs. In this regard, we note that the larger strip of uncertainty in Fig.4(Right) is due to the smearing of the whole bunch of BMS DAs. At this stage of the analysis, one cannot reliably prefer one of these DAs to the other.

C. Estimate of the NLO contribution within FAPT

We have obtained the contribution to $H_{(n)}^{(1)}$ from the pair of diagrams (a, a') in the Feynman gauge,

$$H_{(n)}^{(1)} \Rightarrow H_{(n)}^{(1a)} = H^{(0)}(u) \underset{u}{\otimes} \left[\mathbb{1} + \bar{a}_s(u) \mathcal{H}^{(1a)}(u, v) \right] \left(\frac{\bar{a}_s(u)}{a_s(\mu_0^2)} \right)^{\nu_n} \underset{v}{\otimes} \psi_n(v) . \tag{28}$$

The explicit expression for $T_a^{(1)}$ is presented in (A1) and contains the evolutional log, L(z) accompanied by the V^a part of the ERBL kernel, as was discussed in Sec.II. Refined $\mathcal{H}^{(1a)}$ presented in (A3) reads

$$\bar{a}_s(u)\mathcal{H}^{(1a)}(u,v) = \bar{a}_s(u)C_F U(u,v).$$
 (29)

It should be emphasized that we consider only a part of the NLO contribution related to the "handbag" diagrams here. Substituting (29) in (28), performing the replacements that are due to the dispersion relation

$$\bar{a}_s^{\nu}(u) \to \Delta_{\nu}(s(u), q(u)), \quad \underset{v}{\otimes} \psi_n(v) \to \underset{v}{\otimes} (\theta(v \geqslant v_0)\psi_n(v)), \quad \mathbb{1} = \delta(u - v),$$

and using the notation $\Delta_{\nu}(u) \equiv \Delta_{\nu}(s(u), q(u))$, one arrives to the result of the dispersion relation under $H_{(n)}^{(1a)}$

$$H_{(n)}^{(1a)LCSR} = \frac{1}{a_s^{\nu_n}(\mu_0^2)} H_0(u) \otimes \left\{ \Delta_{\nu_n}(u) \mathbb{1} + \Delta_{(1+\nu_n)}(u) C_F U(u,v) \right\} \otimes (\theta(v \geqslant v_0) \psi_n(v)). \tag{30}$$

Now, we need to perform the Borel transformation under $H_{(n)}^{(1a)LCSR}$ in (30), as was done in Sec.III B. Recall that

$$M^2 \hat{\mathbf{B}} \left[H_0(u) \Delta_{\nu_n}(u) \right] = \left[\mathfrak{A}_{\nu_n} \left(s(u) \right) + \int_0^{s(u)} \rho_{\nu_n}(s) \omega_1(s, u) ds \right] \exp \left(-\frac{Q^2}{M^2} \frac{\bar{u}}{u} \right). \tag{31}$$

So, using Eq.(31) for the transformation of (30), one obtains

$$F_{\pi,n}^{(\text{tw2})\text{LCSR},1a}(Q^2, M^2) = M^2 \hat{\mathbf{B}} H_{(n)}^{(1a)\text{LCSR}} = \frac{1}{a_s^{\nu_n}(\mu_0^2)} \left\{ \left[\mathfrak{A}_{\nu_n}(s(u)) + \int_0^{s(u)} \rho_{\nu_n}(s)\omega_1(s,u)ds \right] \underset{u}{\otimes} \mathbb{1} + C_F \left[\mathfrak{A}_{(\nu_n+1)}(s(u)) + \int_0^{s(u)} \rho_{(\nu_n+1)}(s)\omega_1(s,u)ds \right] \underset{u}{\otimes} U(u,v) \right\} \exp\left(-\frac{Q^2}{M^2} \frac{\bar{u}}{u} \right) \\ \underset{u}{\otimes} (\theta(v \geqslant v_0)\psi_n(v)) . \tag{32}$$

We obtain a NLO estimate of $F_{\pi}^{\text{LCSR}}(Q^2)$ in Eq.(27) replacing the LO $F_{\pi,n}^{(\text{tw2})\text{LCSR},\text{LO}}$ with the partial NLO result $F_{\pi,n}^{(\text{tw2})\text{LCSR},\text{1a}}$. We will consider this result to be *a lower bound* of the emFF in the NLO. The final results at different nonperturbative inputs are presented in Fig.5 with the same notations as in Fig.4.

The predictions presented in both panels of Fig.5, for DA^{bf} (left) and for the bunch of BMSmod (right), respectively, look to be good. But the curves with DA^{bf} in Fig.5(left) look a bit more corresponding to the experimental data in [7]. In addition, the estimate of the upper limit (hybrid) for this case, see Fig.4(left), does not change this correspondence.

VI. CONCLUSIONS

We reconsider the perturbative part of the LCSR for the electromagnetic pion form factor (emFF) by including renormalization group logarithm summation. Together with the dispersion approach inherent in the LCSR, this summation necessarily leads to fractional Analytic Perturbation Theory (FAPT) at the calculation of the emFF.

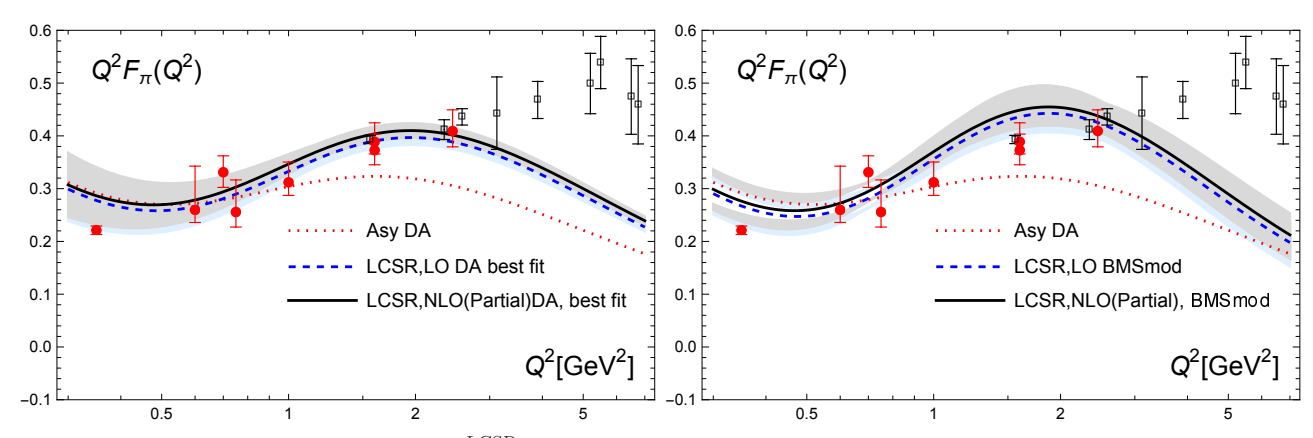


FIG. 5: The predictions for the (partial N)LO F_{π}^{LCSR} , the notations are the same as in Fig.4 in both panels. The red discs with their error bars – experimental data from [7]; the open boxes with bars – recent lattice results [28]. **Left:** Based on DA^{bf} (item (iv)), dashed blue line presents LO, upper solid black line, named "Partial", presents the (partial N)LO corrections in Eq.(32). **Right:** The same designations are for the LO and the (partial N)LO to emFF, based on the bunch of BMSmod DAs (item (i)).

This approach is sequentially applied to twist-2 and twist-4 contributions. It makes the size of radiative corrections effectively smaller and extends the domain of applicability of pQCD to the lower transfer momentum $Q^2 \sim 0.5 \, \mathrm{GeV}^2$.

The results for the pion emFF are the effect of synthesis of FAPT, manifested within the LCSR, and of nonperturbative inputs that are shaped by the intrinsic pion structure in the form of its distribution amplitudes of twist-2, $\varphi_{\pi}^{(2)}(x)$, twist-4, $\varphi_{\pi}^{(4)}(x)$, and twist-6. These nonperturbative characteristics, $\varphi_{\pi}^{(2)}$ and $\delta_{\text{tw-4}}^2$, were established within nonlocal condensate sum rules approach in [19, 24] and [17] respectively, and confirmed within the LCSR analysis of the pion transition form factor in [5, 10].

Our calculation of the emFF shows a good agreement with the experimental data [7], see Fig.5, in spite of the incompleteness of the NLO of the pQCD corrections. The completed NLO calculation for the emFF will allow one to perform the numerical analysis and reliably extract from the experimental data the pion distribution amplitude $\varphi_{\pi}^{(2)}$ of the leading twist.

Acknowledgments

This work was supported in part by FONDECYT (Chile) Grant No. 1240329 (C.A.). S.V.M. is very thankful to Universidad Técnica Federico Santa María, Valparaíso, Chile, where this work was started, for hospitality.

Appendix A: QCD perturbative expansion beyond the leading order

The factorized amplitudes $T^{(1)}$ of the partonic subprocess for $\pi - \gamma$, see Eq.(3b), that correspond to the "handbag" diagrams (a, a') taken in Feynman gauge and presented, e.g., in the first row of Fig.3 in [3] $(\mu_F^2 = \mu_R^2 = \mu^2)$, reads

$$a_s(\mu^2)T_a^{(1)}(y) = a_s(\mu^2)C_F H_0(x) \underset{x}{\otimes} \left\{ L(x) 2V^a(x,y) + \left[\frac{\theta(\bar{y} > \bar{x})}{\bar{y}} - V^a(x,y) \right] \right\}; \tag{A1a}$$

$$a_s(\mu^2)T_{a'}^{(1)}(y) = a_s(\mu^2)C_F H_0(x) \underset{r}{\otimes} [L(x) - 1] \mathbb{1}(x, y);$$
 (A1b)

$$L(x) = \ln\left(\frac{q(x)}{\mu^2}\right); \ q(x) = \sigma x + Q^2 \bar{x}. \tag{A1c}$$

The first term in braces in (A1a) corresponds to the ERBL-evolution logarithm discussed before in Eq.(5); this term is transferred later to the common factor with $(\bar{a}_s(u))^{\nu}$ in Eq.(5). The second term (in square brackets) shapes the term $\bar{a}_s(u)\mathcal{H}^{(1)}(u,v)$ in Eq.(5). The logarithm L(x) in (A1b) (diagram a') is of ultraviolet nature ($\mu = \mu_R$) and cancels

among other diagrams (including renormalization of quark legs) due to the Ward identity. The other diagrams in Fig.3 [3] should lead to the contributions related to the part V^b of the whole kernel V_0 and some remainder. The elements V^a , V^b of the one-loop evolution kernel V_0 are

$$V_0(x,y) = C_F V_+^{(0)}(x,y) \equiv C_F 2 \left[V^a(x,y) + V^b(x,y) \right]_+ = C_F 2 \left[\mathcal{C}\theta(y > x) \frac{x}{y} \left(1 + \frac{1}{y-x} \right) \right]_+; \tag{A2a}$$

$$V^{a}(x,y) = \mathcal{C}\theta(y > x)\frac{x}{y}; \quad V^{b}(x,y) = \mathcal{C}\theta(y > x)\frac{x}{y}\left(\frac{1}{y-x}\right), \tag{A2b}$$

$$V_0(x,y) \otimes \psi_n(y) = C_F 2 \left[V^a(x,y) + V^b(x,y) \right]_+ \otimes \psi_n(y) = -\frac{1}{2} \gamma_0(n) \psi_n(x),$$
 (A2c)

where the symbol \mathcal{C} means $\mathcal{C} = 1 + \{x \to \bar{x}, y \to \bar{y}\}$. Based on (A1) one obtains for the kernel $\mathcal{H}^{(1)}$

$$\mathcal{H}_{a}^{(1)}(u,v) = C_{\rm F} U(u,v), \text{ where } U(u,v) = \frac{\theta(\bar{v} > \bar{u})}{\bar{v}} - V^{a}(u,v).$$
 (A3)

The leading-order coefficient of the β function, and the anomalous dimension $\gamma(n)$ used in the above equations are

$$\frac{d}{dI}\bar{a}_s = -\beta(\bar{a}_s) = -\bar{a}_s^2(\beta_0 + \bar{a}_s\beta_1 + \dots) , \qquad (A4a)$$

$$\beta_0 = \frac{11}{3} C_A - \frac{4}{3} T_R n_f; \ \gamma_0(n) = 2C_F \left[4 \left(\psi(2+n) - \psi(2) \right) - \frac{2}{(n+1)(n+2)} + 1 \right]; \ \nu_n = -\frac{1}{2} \frac{\gamma_0(n)}{\beta_0}, \ (A4b)$$

with n_f being the number of active flavors ($n_f=3$ here) and $T_{\rm R}=1/2, C_{\rm F}=4/3, C_{\rm A}=N_c=3$ for ${\rm SU}_c(3)$.

Appendix B: FAPT coupling constants and their properties

In this Appendix, we give the expressions for the standard one-loop running couplings and their FAPT counterparts. To facilitate the representation, we express them in terms of the auxiliary variables $L = \ln(Q^2/\Lambda_{\rm QCD}^2)$, $L_s = \ln(s/\Lambda_{\rm QCD}^2)$, multiplied for simplicity by the term β_0^{ν} . In other words, we shift the origin of the different coupling images to the values $a_s \to A_s = \beta_0 a_s = \beta_0 \alpha_s/(4\pi)$, the corresponding auxiliary FAPT coupling constants are shown with the symbol "bar", $\bar{A}_{\nu} = \beta_0^{\nu} A_{\nu}$, $\bar{\mathfrak{A}}_{\nu} = \beta_0^{\nu} \mathfrak{A}_{\nu}$, $\bar{\mathfrak{A}}_{\nu}$

1. The "minimal" FAPT coupling constants $A_{\nu}, \mathfrak{A}_{\nu}$ at one-loop running

The properties of the "minimal" FAPT couplings constants at one-loop running with L and L_s reads,

$$A_s^{\nu}[L] = \frac{1}{L^{\nu}}$$
 standard pQCD, (B1a)

$$\bar{\mathcal{A}}_{\nu}[L] = \frac{1}{L^{\nu}} - \frac{F(e^{-L}, 1 - \nu)}{\Gamma(\nu)};$$
 $\bar{\mathcal{A}}_{1}[L] = \frac{1}{L} - \frac{1}{e^{L} - 1},$ spacelike FAPT, (B1b)

$$\bar{\mathcal{A}}_0[L] = 1; \quad \bar{\mathcal{A}}_{0 < \nu < 1}[L \to -\infty] \to |L|^{1-\nu}; \quad \bar{\mathcal{A}}_1[L \to -\infty] \to 1; \quad \bar{\mathcal{A}}_{\nu > 1}[L \to -\infty] \to 0,$$
 (B1c)

$$\bar{\mathfrak{A}}_{\nu}[L_s] = \frac{\sin\left[(\nu - 1)\phi\right]}{\pi\left(\nu - 1\right)\left(L_s^2 + \pi^2\right)^{(\nu - 1)/2}}; \quad \bar{\mathfrak{A}}_1[L_s] = \frac{\phi}{\pi}; \quad \phi = \arccos\left(\frac{L_s}{\sqrt{L_s^2 + \pi^2}}\right), \quad \text{timelike FAPT}, \quad (B1d)$$

$$\bar{\mathfrak{A}}_0[L_s] = 1; \quad \bar{\mathfrak{A}}_{0<\nu<1}[L_s \to -\infty] \to \left(\sqrt{L_s^2 + \pi^2}\right)^{1-\nu}; \quad \bar{\mathfrak{A}}_1[L_s \to -\infty] \to 1; \quad \bar{\mathfrak{A}}_{\nu>1}[L_s \to -\infty] \to 0. \tag{B1e}$$

where the symbol [L] is used to denote the function argument, clearly distinguishing it from the Q^2 dependence.² In Eq.(B1b) there appears the "pole remover" $\frac{F(e^{-L},1-\nu)}{\Gamma(\nu)}$ – to the standard $A_s^{\nu}(L)$, it is expressed in terms of the Lerch transcendental function, or is $\frac{\text{Li}_{(1-\nu)}(e^{-L})}{\Gamma(\nu)}$, $F(z,\nu)=\text{Li}_{\nu}(z)$ [12].

It is seen that the couplings $\bar{\mathcal{A}}_{\nu}[L]$, $\bar{\mathfrak{A}}_{\nu}[L]$ become unbounded in the vicinity of $Q^2=0$ and $0<\nu\leqslant 1$. It can be interpreted as that the well-known singularity of the standard running coupling $A_s^{\nu}[L]$ in Eq. (B1a) at $L=0(Q^2=\Lambda^2)$ and $\nu>0$ turns into a singularity of the FAPT couplings in the limit $L\to-\infty$ for $0<\nu<1$, cf. (B1c) and (B1e). Therefore, these results for $\bar{\mathcal{A}}_{\nu}[L]$, $\bar{\mathfrak{A}}_{\nu}[L]$ cannot be directly used in the vicinity of $Q^2=0$ and $0<\nu\leqslant 1$, where the FAPT couplings are ill-defined. We redefine these couplings in this regime by demanding that they vanish together with its first derivatives. This intervention guarantees, among other things, that observables calculated with them, e.g., the pion form factors [5, 9, 11], have the correct UV asymptotics following from pQCD. To this end, we redefine the couplings $\bar{\mathcal{A}}_{\nu}$, $\bar{\mathfrak{A}}_{\nu}$ in the vicinity of $Q^2=0$

and, for
$$0 < \nu \le 1$$
: $\bar{\mathcal{A}}_{\nu}[-\infty] = 0$, $\bar{\mathcal{A}}'_{\nu}[-\infty] = 0$, $\bar{\mathfrak{A}}'_{\nu}[-\infty] = 0$, $\bar{\mathfrak{A}}'_{\nu}[-\infty] = 0$, (B2)

while the behavior of these couplings for $\nu > 1$ remains unaffected. It should be mentioned that the constraints like (B2) can be realized in the modeling of low-energy behavior following the way [31, 32]. We prefer to avoid the models here; instead, we formulate these constraints at the point $Q^2 = 0$ explicitly. Simultaneously, we hope that the integration over this vicinity does not contribute significantly.

2. Spectral density ρ_{ν} and coupling \mathcal{I}_{ν}

The auxiliary spectral density $\bar{\rho}_{\nu}$ has the form $(L_{\sigma} = \ln(\sigma/\Lambda_{\rm QCD}^2))$,

$$\bar{\rho}_{\nu}(\sigma) = \bar{\rho}_{\nu}[L_{\sigma}] \equiv \beta_0^{\nu} \rho_{\nu}[L_{\sigma}] = \frac{1}{\pi} \operatorname{Im} \left[A^{\nu}(-\sigma) \right] \xrightarrow{\text{1-loop}} \frac{1}{\pi} \frac{\sin \left[\nu \phi \right]}{\left(L_{\sigma}^2 + \pi^2 \right)^{\nu/2}}, \quad \bar{\rho}_1[L_{\sigma}] = \frac{1}{L_{\sigma}^2 + \pi^2}, \tag{B3}$$

see the definitions of A^{ν} in (B1a) and ρ_{ν} in (10a). The $\bar{\rho}_{\nu}(\sigma)$ is the origin of FAPT coupling constants

$$\bar{\mathcal{A}}_{\nu}(x) = \int_{0}^{\infty} \frac{d\sigma}{\sigma + x} \bar{\rho}_{\nu}(\sigma) , \quad \bar{\mathfrak{A}}_{\nu}(y) = \int_{y}^{\infty} \frac{d\sigma}{\sigma} \bar{\rho}_{\nu}(\sigma) , \qquad (B4)$$

presented in the one-loop approximation in Eqs.(B1b,B1d). All of the invented coupling constants, $\{A_s^{\nu}, \bar{\mathcal{A}}_{\nu}, \bar{\mathfrak{A}}_{\nu}, \bar{\mathfrak{A}}_{\nu}, \bar{\rho}_{\nu}\}$ satisfy the one-loop RG equation that we show below for the partial case of $\bar{\rho}_{\nu}$

$$\frac{d}{dL}\bar{\rho}_{\nu}[L] = -\nu\,\bar{\rho}_{\nu+1}[L]\,. \tag{B5}$$

The generalized FAPT coupling \mathcal{I}_{ν} is the function of two arguments; it appears due to the action of "subtraction of continuum" ³ and reads

$$\bar{\mathcal{I}}_{\nu}(y,x) = \int_{y}^{\infty} \frac{ds}{s+x} \bar{\rho}_{\nu}(s) = \begin{cases}
\left[\bar{\mathfrak{A}}_{\nu}(y) - x \int_{y}^{\infty} \frac{ds}{s(s+x)} \bar{\rho}_{\nu}(s)\right] \leqslant \bar{\mathfrak{A}}_{\nu}(y) \text{ (for } \bar{\rho}_{\nu} \geqslant 0), \\
\left[\bar{\mathcal{A}}_{\nu}(x) - \int_{0}^{y} \frac{ds}{s+x} \bar{\rho}_{\nu}(s)\right] \leqslant \bar{\mathcal{A}}_{\nu}(x) \text{ (for } \bar{\rho}_{\nu} \geqslant 0),
\end{cases}$$
(B6)

$$\bar{\mathcal{I}}_{\nu}(y,0) = \bar{\mathfrak{A}}_{\nu}(y), \quad \bar{\mathcal{I}}_{\nu}(0,x) = \bar{\mathcal{A}}_{\nu}(x), \quad \bar{\mathcal{I}}_{1}(0,0) = \bar{\mathfrak{A}}_{1}(0) = \bar{\mathcal{A}}_{1}(0).$$
 (B7)

² An expression analogous to (B1d) was derived long ago in [29, 30] in connection with multiloop calculations and the Higgs-boson decay into hadrons.

³ It should be mentioned that $\mathcal{I}_1(y,x)$ also appeared in [32, 33] due to the modeling of spectral density $\rho_1(s)$ at low energy.

The coupling $\mathcal{I}_{\nu}(y,x)$ is regular for y>0, x>0, while for y=0 or x=0 it reduces to the initial FAPT couplings in accordance with Eq. (B7). For the important case $\nu=1$, the expression for $\bar{\mathcal{I}}_1(y,x)$ reduces to

$$\bar{\mathcal{I}}_1(y,x) = \frac{1}{L_x} - \frac{1}{e^{L_x} - 1} - \int_0^y \frac{ds}{s+x} \left(\frac{1}{L_s^2 + \pi^2}\right),\tag{B8}$$

where $L_x = \ln(x/\Lambda^2)$, e.g.,

$$\bar{\mathcal{A}}_{1}(\Lambda^{2}) = \bar{\mathfrak{A}}_{1}(\Lambda^{2}) = \frac{1}{2} > \bar{\mathcal{I}}_{1}(\Lambda^{2}, \Lambda^{2}) \simeq \bar{\mathcal{A}}_{1}(\Lambda^{2}) - 0.06 \approx \bar{\mathcal{A}}_{1}(\Lambda^{2}) - \left(\frac{\ln(2)}{\pi^{2}} - \frac{3}{4}\frac{\zeta_{3}}{\pi^{4}}\right)$$
(B9)

3. Extended boundary conditions

For the twist-4 contribution, see Eq.(23), we face with a new effective coupling constant $\bar{\mathcal{I}}'_{\nu}(s(u),0)$

$$\bar{\mathcal{I}}'_{\nu}(s(u),0) \equiv \frac{d}{dx}\bar{\mathcal{I}}_{\nu}(y,x)\Big|_{x=0} = -\int_{s(u)}^{\infty} \frac{ds}{s^2}\bar{\rho}_{\nu}(s), \qquad (B10a)$$

that enters later into the convolution with $\varphi(u) = \varphi_{\pi}^{(4)}(u)e^{\left(-\frac{Q^2}{M^2}\frac{\bar{u}}{u}\right)}/u$. The application to the last term in (B10a) sequentially integrating by parts and the usage of (B5) leads to the representation

$$\int_{s(u)}^{\infty} \frac{ds}{s^2} \bar{\rho}_{\nu}(s) = \left(\frac{\bar{\rho}_{\nu}(s(u))}{s(u)} - \nu \frac{\bar{\rho}_{\nu+1}(s(u))}{s(u)} + \nu(\nu+1) \int_{s(u)}^{\infty} \frac{ds}{s^2} \bar{\rho}_{\nu+2}(s)\right) = \sum_{n=0} (-1)^n \frac{\Gamma(\nu+n)}{\Gamma(\nu)} \frac{\bar{\rho}_{\nu+n}(s(u))}{s(u)}, \text{(B10b)}$$
and
$$\frac{\bar{\rho}_{\nu+n}(s)}{s} = \frac{e^{-\pi t}}{\pi^{(1+\nu+n)}} \frac{\sin[(\nu+n)\phi]}{(1+t^2)^{(\nu+n)/2}}, \ \phi = \arccos\left(\frac{t}{\sqrt{1+t^2}}\right), \tag{B10c}$$

where $t = \ln(s/\Lambda^2)/\pi$, $s(u) = (s_0 + Q^2)(u - u_0)$. In other words, we expanded $\bar{\mathcal{I}}'_{\nu}(s(u), 0)$ in (B10a) in a series in the standard coupling constants $\bar{\mathfrak{A}}'_{\nu+n}(s(u))$. Every term in the sum in the rhs of Eq.(B10b), starting with the second one at n = 1, is integrable over u, while the first term, $-\frac{\bar{\rho}_{\nu}(s)}{s} = \frac{d}{ds}\bar{\mathfrak{A}}_{\nu}(s)\Big|_{s=s(u)}$, is nonintegrable per se due to the inclusion of the vicinity of $s(u_0) = 0$. Nevertheless, taking the corresponding integral in (20) by part and using the condition (B2) for the "surface term", one obtains

$$\int_{u_0}^1 \bar{\mathfrak{A}}'_{\nu+n}(s(u)) \varphi(u) du = 0 - \int_0^{s_0} \bar{\mathfrak{A}}_{\nu+n}(s) \varphi'\left(\frac{Q^2 + s}{Q^2 + s_0}\right) \frac{ds}{(Q^2 + s_0)^2}, \tag{B11}$$

where the integral in the rhs is convergent even at n = 0. One can use a few (two) first terms in the expansion (B10b), which is enough for our NLO calculation accuracy. The final expression for the integration of $\bar{\mathcal{I}}'_{\nu}(s(u),0)$ based on (B11) and as applied to Eq.(23) reads

$$\int_{u_0}^1 \mathcal{I}'_{\nu_{t4}}(s(u), 0)\varphi(u)du = -\frac{1}{(\beta_0)^{\nu_{t4}}} \int_0^{s_0} \left(\bar{\mathfrak{A}}_{\nu_{t4}}(s) + \sum_{n=1} (-1)^n \frac{\Gamma(\nu+n)}{\Gamma(\nu)} \bar{\mathfrak{A}}_{(\nu_{t4}+n)}(s) \right) \varphi'\left(\frac{Q^2+s}{Q^2+s_0} \right) \frac{ds}{(Q^2+s_0)^2}$$
(B12)

Appendix C: Borel transformation

We used the standard form of the Borel transform for QCD SR, see e.g. in [34], it reads $\hat{\mathbf{B}}_{(M^2 \to \sigma)}[f(\sigma)]$ and manifests itself as the limit of a series of derivatives of the function $f(\sigma)$

$$\hat{\mathbf{B}}_{(M^2 \to \sigma)}[f(\sigma)] \equiv \hat{\mathbf{B}}[f(\sigma)](M^2) \stackrel{def}{=} \lim_{\substack{\sigma = nM^2 \\ n \to \infty}} \frac{(-\sigma)^n}{\Gamma(n)} \frac{\mathrm{d}^n}{\mathrm{d}\sigma^n} [f(\sigma)]. \tag{C1}$$

Further, for shortness, we will omit the subscript at $\hat{\mathbf{B}}_{(M^2 \to \sigma)} \equiv \hat{\mathbf{B}}$.

$$\hat{\mathbf{B}}\left[\exp\left(-\sigma a\right)\right] = \delta\left(1 - M^2 a\right). \tag{C2}$$

Based on (C2), one can derive

$$\hat{\mathbf{B}}\left[\left(\frac{1}{\sigma}\right)^{\nu}\right] = \frac{1}{\Gamma(\nu)} \left(\frac{1}{M^2}\right)^{\nu}, \ \hat{\mathbf{B}}\left(\frac{1}{\sigma + Q^2}\right)^{\nu} = e^{-\frac{Q^2}{M^2}} \frac{1}{\Gamma(\nu)} \left(\frac{1}{M^2}\right)^{\nu}. \tag{C3}$$

For the σ -dependence in (22), where $x = q(u) = \sigma u + Q^2 \bar{u}$, one obtains

$$M^2 \hat{\mathbf{B}} \left[\frac{u}{q(u)} \right] = e^{-\frac{Q^2}{M^2}} \frac{\bar{u}}{u}; \tag{C4a}$$

$$M^2 \hat{\mathbf{B}} \left[\frac{u}{(s+q(u)) q(u)} \right] = \frac{1}{s} \left[1 - \exp\left(-\frac{s}{M^2 u}\right) \right] e^{-\frac{Q^2}{M^2}} \frac{\bar{u}}{u}; \tag{C4b}$$

$$M^{2}\hat{\mathbf{B}}\left[\frac{u}{(s+q(u))\,q(u)^{2}}\right] = \frac{1}{s^{2}}\left[\exp\left(-\frac{s}{M^{2}u}\right) - \left(1 - \frac{s}{M^{2}u}\right)\right]e^{-\frac{Q^{2}}{M^{2}}}\frac{\bar{u}}{u}.$$
 (C4c)

The Borel transform of one-loop QCD running $\bar{a}_s(q(u)) = \frac{1}{b_0 \ln(q(u)/\Lambda^2)}$

$$M^2 \hat{\mathbf{B}} \left[\bar{a}_s^{\nu}(q(u)) \right] = M^2 \exp\left(-\frac{Q^2}{M^2} \frac{\bar{u}}{u} \right) \frac{\nu}{b_0^{\nu}} \boldsymbol{\mu} \left(\frac{\Lambda^2}{uM^2}, \nu \right) ; \tag{C5a}$$

$$M^2 \hat{\mathbf{B}} \left[\bar{a}_s^{\nu}(q(u)) \frac{u}{q(u)} \right] = \exp\left(-\frac{Q^2}{M^2} \frac{\bar{u}}{u} \right) \frac{1}{b_0^{\nu}} \boldsymbol{\mu} \left(\frac{\Lambda^2}{uM^2}, \nu - 1 \right); \tag{C5b}$$

where
$$\mu(t,\nu) = \int_0^\infty dx \frac{x^\nu}{\Gamma(\nu+1)} \frac{t^x}{\Gamma(x+1)}$$
. (C5c)

The Borel images of \bar{a}_s^{ν} in Eq.(C5) are new results. It should be mentioned that the behavior of these images in (C5) does not correspond to the behavior of $\bar{a}_s^{\nu}(\mu_u^2) = \bar{a}_s^{\nu}(M^2u + Q^2\bar{u})$, where the ansatz

$$\mu^2 \to \mu_u^2 = M^2 u + Q^2 \bar{u}$$
 (C6)

was suggested in [3] and used in [3, 4, 6].

Appendix D: Higher twist contributions

The explicit expressions for the twist-4 [4] amplitude $H_{\pi}^{(4)}$ read

$$H_{\pi}^{(4)}(Q^2) = \int_0^{s_0} \frac{ds'}{s' + \sigma} \rho_{\text{tw-4}}(s'); \ \rho_{\text{tw-4}}(s') = \frac{\delta_{\text{tw-4}}^2(\mu^2)}{u^2} \frac{d}{ds'} \delta\left(\frac{\bar{u}}{u} Q^2 - s'\right) \otimes (u\varphi^{(4)}(u))$$
 (D1)

$$H_{\pi}^{(4)}(Q^2) = \delta_{\text{tw-4}}^2(\mu^2) \left[\frac{\theta(u > u_0)}{\left(u\sigma + \bar{u}Q^2\right)^2} + \frac{\delta(u - u_0)}{\left(u\sigma + \bar{u}Q^2\right)} \frac{1}{s_0 + Q^2} \right] \otimes \left(u\varphi_{\pi}^{(4)}(u)\right)$$
 (D2)

$$= \delta_{\text{tw-4}}^{2}(\mu^{2}) \left[\int_{u_{0}}^{1} du \frac{\varphi_{\pi}^{(4)}(u)}{u \left(\sigma + \frac{\bar{u}}{u}Q^{2}\right)^{2}} + \frac{\varphi_{\pi}^{(4)}(u_{0})}{\sigma + \frac{\bar{u}}{u}Q^{2}} \frac{u_{0}}{Q^{2}} \right], \tag{D3}$$

where $u_0 = \frac{Q^2}{Q^2 + s_0}$, $\bar{u}_0 = \frac{s_0}{Q^2 + s_0}$. Applying the Borel transform $M^2\hat{\mathbf{B}}$ to the amplitude $H_{\pi}^{(4)}$, one obtains [4]

$$F_{\pi}^{(4)}(Q^2, M^2) = M^2 \hat{\mathbf{B}} \left[H_{\pi}^{(4)}(Q^2, \sigma) \right] = \delta_{\text{tw-4}}^2(\mu^2) \left[\int_{u_0}^1 du \frac{\varphi_{\pi}^{(4)}(u)}{uM^2} e^{-\frac{\bar{u}}{u} \frac{Q^2}{M^2}} + \varphi_{\pi}^{(4)}(u_0) \frac{u_0}{Q^2} e^{-\frac{s_0}{M^2}} \right], \tag{D4}$$

To estimate $\delta_{\text{tw-4}}^2(\mu_0^2=1\,\text{GeV}^2)$ it was related to λ_q^2 using QCD SR approach in [17]. The numerical estimate is $\delta_{\text{tw-4}}^2(\mu_0^2=1\,\text{GeV}^2)\approx \lambda_q^2/(2\cdot 1.075)=(0.4-0.45)/(2\cdot 1.075)\approx 0.198\pm 0.02\,\text{GeV}^2$. The common factor $\delta_{\text{tw-4}}^2(\mu^2)$ should be transferred under the integral in the rhs of (D2) when applying the ansatz $\mu^2=M^2u+Q^2\bar{u}$.

Appendix E: Pion DAs of twist-2

The parametric presentation (b_2, b_4) for different pion DAs in Fig.6 is taken from [5]; and some of corresponding profiles of pion DAs presented in Fig.6 are shown in Fig.7. Both the BMSmod \blacktriangle and the platykurtic DA \clubsuit belong to the 1σ level (red ellipse) of the best-fit point DA^{bf} \bullet .

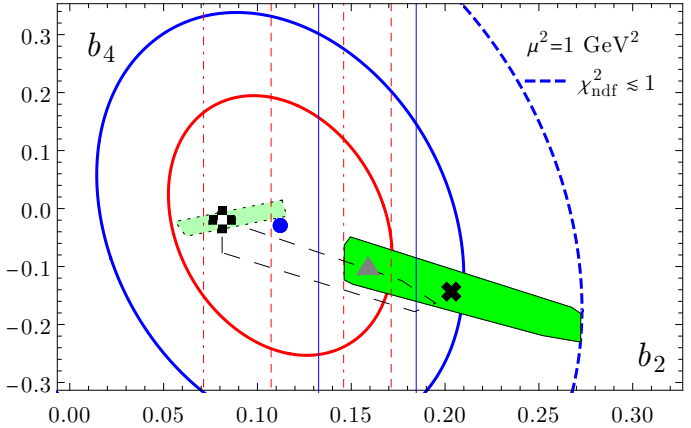


FIG. 6: (color in line) The conformal expansion coefficients b_2, b_4 are on the axes. The following notations are used: black ***** is BMS DA [19]; black/white \bullet is the platykurtic DA [26, 35]; DAmod is shown as a grey \blacktriangle (0.159 $^{+0.025}_{-0.027}$, -0.098 $^{+0.05}_{-0.03}$) selected from the BMS set of DAs to be inside the 1σ error ellipse (innermost red line), while vertical solid lines are the N³LO lattice constraints on b_2 from lattice QCD [36]. Results of the fitting procedure for the twist-two conformal coefficients b_2, b_4 with fixed higher-twist parameters is shown as blue best fit \bullet - ($b_2^{bf} = 0.112, b_4^{bf} = -0.029$). Two rectangles along the lower diagonal denote the range of (b_2, b_4) determined within the BMS approach [19] for two different values of $\lambda_q^2 = 0.4$ GeV² (larger shaded rectangle) and 0.45 GeV² (transparent rectangle), where the BMS DA [19] is represented by *****. The smaller shaded rectangle encloses the range of (b_2, b_4) coefficients associated with DAs having a platykurtic profile [26], like the model \bullet proposed in [35]. The dash-dotted, dashed (red), and solid (blue) vertical lines show the lattice results for b_2 from [36] for the NLO (0.109(37)), NNLO (0.139(32)), and N³LO (0.159 $^{+0.025}_{-0.027}$), respectively.

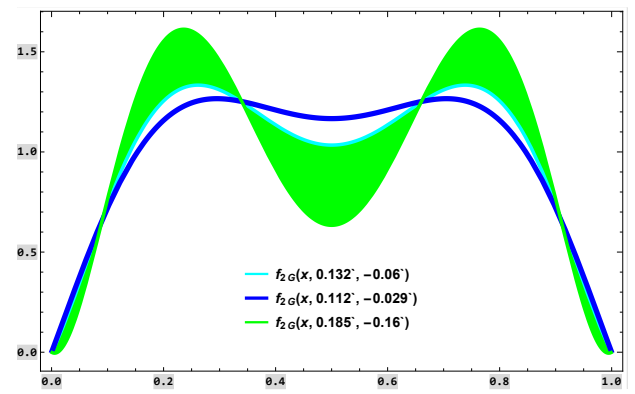


FIG. 7: (color in line) The profiles of different DAs: a bunch of green color is the admissible domain for BMSmod DA \blacktriangle , while the curve navy in color corresponds to the best fit DA \bullet ($b_2^{bf}=0.112, b_4^{bf}=-0.029$) for the pion TFF, compared with the profile of the DA obtained in the lattice approach LaMET in [27].

^[1] A. V. Efremov and A. V. Radyushkin, Phys. Lett. **B94**, 245 (1980).

^[2] A. Khodjamirian, Eur. Phys. J. C6, 477 (1999), hep-ph/9712451.

^[3] V. M. Braun, A. Khodjamirian, and M. Maul, Phys. Rev. D 61, 073004 (2000), hep-ph/9907495.

^[4] J. Bijnens and A. Khodjamirian, Eur. Phys. J. C 26, 67 (2002), hep-ph/0206252.

S. V. Mikhailov, A. V. Pimikov, and N. G. Stefanis, Phys. Rev. D 103, 096003 (2021), 2101.12661.

^[6] S. Cheng, A. Khodjamirian, and A. V. Rusov, Phys. Rev. D 102, 074022 (2020), 2007.05550.

- [7] G. M. Huber, H. P. Blok, T. Horn, E. J. Beise, D. Gaskell, D. J. Mack, V. Tadevosyan, J. Volmer, D. Abbott, K. Aniol, et al. (The Jefferson Lab F_{π} Collaboration), Phys. Rev. C 78, 045203 (2008),
- [8] A. Khodjamirian, T. Mannel, N. Offen, and Y. M. Wang, Phys. Rev. D 83, 094031 (2011), 1103.2655.
- [9] C. Ayala, S. V. Mikhailov, and N. G. Stefanis, Phys. Rev. D 98, 096017 (2018), [Erratum: Phys. Rev. D 101, 059901 (2020)], 1806.07790.
- [10] C. Ayala, S. V. Mikhailov, A. V. Pimikov, and N. G. Stefanis, EPJ Web Conf. 222, 03017 (2019), 1911.02845.
- [11] S. Mikhailov, A. Pimikov, and N. G. Stefanis, EPJ Web Conf. 258, 03003 (2022), 2111.12469.
- [12] A. P. Bakulev, S. V. Mikhailov, and N. G. Stefanis, Phys. Rev. D72, 074014 (2005), [Erratum: Phys. Rev. D72, 119908 (2005)], hep-ph/0506311.
- [13] A. P. Bakulev, S. V. Mikhailov, and N. G. Stefanis, Phys. Rev. D75, 056005 (2007), [Erratum: Phys. Rev. D77, 079901 (2008)], hep-ph/0607040.
- [14] S. V. Mikhailov and N. G. Stefanis, Nucl. Phys. B821, 291 (2009), 0905.4004.
- [15] S. S. Agaev, V. M. Braun, N. Offen, and F. A. Porkert, Phys. Rev. D83, 054020 (2011), 1012.4671.
- [16] S. V. Mikhailov, A. V. Pimikov, and N. G. Stefanis, Phys. Rev. D93, 114018 (2016), 1604.06391.
- [17] A. P. Bakulev, S. V. Mikhailov, and N. G. Stefanis, Phys. Rev. D67, 074012 (2003), hep-ph/0212250.
- [18] A. P. Bakulev and S. V. Mikhailov, Mod. Phys. Lett. A 11, 1611 (1996), hep-ph/9512432.
- [19] A. P. Bakulev, S. V. Mikhailov, and N. G. Stefanis, Phys. Lett. B508, 279 (2001), [Erratum: Phys. Lett. B590, 309 (2004)], hep-ph/0103119.
- [20] A. P. Bakulev, A. V. Pimikov and N. G. Stefanis, Phys. Rev. D 79, 093010 (2009), 0904.2304 [hep-ph].
- [21] G. S. Bali, V. Braun, S. Collins, A. Schäfer, and J. Simeth (RQCD), JHEP 08, 137 (2021), 2106.05398.
- [22] A. P. Bakulev, S. V. Mikhailov, and N. G. Stefanis, Annalen Phys. 13, 629 (2004), hep-ph/0410138.
- [23] W. Detmold, A. V. Grebe, I. Kanamori, C. J. D. Lin, R. J. Perry, and Y. Zhao (HOPE), in 40th International Symposium on Lattice Field Theory (2023), 2311.01322.
- [24] S. V. Mikhailov and A. V. Radyushkin, Sov. J. Nucl. Phys. 49, 494 (1989), Yad. Fiz. 49, 794 (1988), JINR-P2-88-103 (in Russian), URL http://inspirehep.net/record/262441/files/JINR-P2-88-103.pdf.
- [25] S. V. Mikhailov and A. V. Radyushkin, Phys. Rev. **D45**, 1754 (1992).
- [26] N. G. Stefanis and A. V. Pimikov, Nucl. Phys. A945, 248 (2016), 1506.01302.
- [27] E. Baker, D. Bollweg, P. Boyle, I. Cloët, X. Gao, S. Mukherjee, P. Petreczky, R. Zhang, and Y. Zhao, JHEP 07, 211 (2024), 2405.20120.
- [28] H.-T. Ding, X. Gao, A. D. Hanlon, S. Mukherjee, P. Petreczky, Q. Shi, S. Syritsyn, R. Zhang, and Y. Zhao, Phys. Rev. Lett. 133, 181902 (2024), 2404.04412.
- [29] S. G. Gorishnii, A. L. Kataev, and S. A. Larin, Sov. J. Nucl. Phys. 40, 329 (1984), [Yad. Fiz. 40, 517 (1984)].
- [30] D. J. Broadhurst, A. L. Kataev, and C. J. Maxwell, Nucl. Phys. B592, 247 (2001), hep-ph/0007152.
- [31] C. Ayala, G. Cvetič, and R. Kögerler, J. Phys. G44, 075001 (2017), 1608.08240.
- [32] C. Ayala, G. Cvetič, R. Kögerler, and I. Kondrashuk, J. Phys. G45, 035001 (2018), 1703.01321.
- [33] C. Ayala and G. Cvetic, JHEP 12, 075 (2024), 2410.00220.
- [34] M. A. Shifman, A. I. Vainshtein, and V. I. Zakharov, Nucl. Phys. B147, 385 (1979).
- [35] N. G. Stefanis, Phys. Lett. **B738**, 483 (2014), 1405.0959.
- [36] G. S. Bali, V. M. Braun, S. Bürger, M. Göckeler, M. Gruber, F. Hutzler, P. Korcyl, A. Schäfer, A. Sternbeck, and P. Wein, JHEP 08, 065 (2019), [Addendum: JHEP 11, 037 (2020)], 1903.08038.